Master sintering curve and microstructure evolution of perovskite layer structured $La_2Ti_2O_7$ ceramics

Kaustubh R. Kambale[1,*], Eliza Malhotra[1], Jagmohan D. Sharma[1], Ajit R. Kulkarni[2], Narayanan Venkataramani[2], Krutika Rasal[3], Sandeep P. Butee[3]

[1]*Department of Metallurgical and Materials Engineering, Punjab Engineering College (Deemed to be University), Chandigarh, Sector 12, Chandigarh – 160012, India*

[2]*Department of Metallurgical Engineering and Materials Science, Indian Institute of Technology Bombay, Powai, Mumbai – 400076, India*

[3]*Department of Metallurgy and Materials Engineering, COEP Technological University (A Unitary Public University of Government of Maharashtra), Wellesley Road, Shivaji Nagar, Pune – 411005, India*

Received 2 November 2025; received in revised form 8 February 2026; accepted 16 February 2026

Abstract

The master sintering curve (MSC) theory is one of the widely used theories to predict the densification behaviour of a given powder and green body irrespective of its thermal history. In this paper, MSC was constructed for a high Curie temperature piezoelectric, $La_2Ti_2O_7$. Powder synthesis was carried out by the solid state reaction method, followed by uniaxial pressing to obtain green compacts. Dilatometric shrinkage study of green compacts was carried out up to 1450 °C with heating rates of 5, 10 and 15 °C/min. The apparent activation energy of sintering was found to be 1027 kJ/mol. The results of the present study can be used to predict the densification level obtained during pressureless sintering of the $La_2Ti_2O_7$ powders synthesised by the solid-state method.

***Keywords**: master sintering curve, solid-state synthesis, piezoelectric, powders*

I. Introduction

The concept of master sintering curve (MSC) was proposed by Su and Johnson [1] in order to predict the densification of powder compacts under arbitrary time-temperature excursions. Another important outcome of such a study is to establish the apparent activation energy of sintering for a material under consideration. Since then concept of MSC has been applied successfully to various ceramics and alloys produced by the powder metallurgy route [2–7]. It has been criticised that even though the apparent activation energy of sintering can be determined while constructing the master sintering curve is merely a fitting parameter and should not be regarded as the sintering activation energy [8]. Multiple density-temperature curves can indeed be fitted into a single curve, i.e. master sintering curve, by estimating an apparent activation energy of sintering correctly and therefore, an apparent activation energy of sintering determined during construction of the master sintering curve can be regarded as a fitting parameter. However, for a given process if the powder characteristics (viz. particle size, particle size distribution, etc.) are same across various batches and the initial (green) density of compacts undergoing sintering is the same and if low heating rates are not chosen while constructing master sintering curve to avoid the surface diffusion (which is a non-densifying mechanism) then one is bound to get same apparent activation energy of sintering for a given material for different batches. While the theory of master sintering curve is not flawless since it assumes that densification occurs through only one diffusion mechanism and an apparent activation energy does not provide any clue about the diffusion mechanism involved in sintering, still it is the most practical tool to predict densification of a powder compact as a function of time and temperature.

The master sintering curve is established by employing constant-rate heating method using a dilatometer whereas its validation is typically done by isothermal sintering of powder compacts. In this process, any observed deviation in terms of density for a given time and temperature can be correlated to

*Corresponding author: tel: +91 7776054446
e-mail: *kaustubhrameshkambale@pec.edu.in*

deviation from the basic assumptions of the master sintering curve theory (e.g. exaggerated grain growth, surface diffusion, etc.). Assuming that only one diffusion mechanism, i.e. either volume diffusion or grain boundary diffusion, dominates during the entire process of sintering and microstructure is dependent only on density, the MSC can be constructed by the following equation:

$$\Theta(t,T)=\int_{t_0}^{t}\frac{1}{T}\exp\left(-\frac{Q}{RT}\right)dt \qquad (1)$$

where Q is apparent activation energy of sintering, R is universal gas constant, t is time and T is absolute temperature [1].

$La_2Ti_2O_7$ is a piezoceramic belonging to the perovskite layer structure (PLS) family exhibiting Curie temperature (T_C) of about 1460 °C [9]. In fact, it is one of the few piezoceramics exhibiting T_C greater than 1000 °C. As a rule of thumb, the usage temperature of piezoceramics is ½ of T_C. Therefore, $La_2Ti_2O_7$ is considered as one of the candidate materials useful for sensors applications which can be used for structural health monitoring of next generation aerospace and aircraft engines, nuclear power plants etc. where service temperature is above 500 °C [10]. It should be noted that even though T_C of $La_2Ti_2O_7$ was established way back in 1974 by Nanamatsu *et al*. [9], various aspects related to the processing of these ceramics, especially those related to sintering have not been adequately addressed. Some of the earlier research on these ceramics have reported pressureless sintering of powders synthesized by different routes. Recent focus with the respect to sintering has shifted to the fabrication of textured ceramics [11–13]. However, it needs to be taken into account that since $La_2Ti_2O_7$ exhibits monoclinic structure and 95% of single crystal polarization is achievable in polycrystalline ceramics, there is little advantage of fabricating textured ceramics using techniques such as spark plasma sintering (SPS), SPS followed by hot pressing (HP), sintering by applying magnetic field, etc. [14,15].

Therefore, this research article focuses on the fabrication of $La_2Ti_2O_7$ ceramics by conventional pressureless sintering and establish the master sintering curve and grain growth in these ceramics. It should be noted that, irrespective of the sintering technique used to fabricate the ceramics, no literature is available about the master sintering curve of $La_2Ti_2O_7$ ceramics and associated nuances such as onset of sintering temperature, apparent activation energy of sintering and possible insights about the diffusion mechanism responsible.

II. Experimental

Raw materials, used for preparation of $La_2Ti_2O_7$ ceramics, were La_2O_3 (Sigma Aldrich) and TiO_2, predominantly rutile (Sigma Aldrich). Because of hygroscopic nature of La_2O_3, it was first heated to 950 °C for 12 h to remove the moisture. Then, the powders were dispersed in ethanol medium with a ball:powder ratio of 5:1. After milling, slurry was heated in an oven at about 120 °C to remove ethanol. After drying, the dried mass was crushed in agate mortar and pastel and the powder so obtained was fired at 1150 °C for 4 h to obtain single phase monoclinic $La_2Ti_2O_7$ powder. To identify the phases present in the calcined powder, X-ray diffraction was carried out using an X-ray diffractometer (Bruker D8 Advance with Da Vinci Design, Germany) in the 2θ range of 5–90°. X-ray source was Cu-K_α with a wavelength of 1.54 Å. TOPAS software was used for Rietveld refinement.

Before sintering, the calcined $La_2Ti_2O_7$ powders were pressed into pellet form by using 3 wt.% poly vinyl alcohol (PVA) as a binder using a hydraulic press. The powder was pressed under a pressure of 250 MPa for 2 min. To establish the MSC, green $La_2Ti_2O_7$ pellets were subjected to constant rate heating (with heating rates of 5, 10 and 15 °C/min) in a high temperature dilatometer (TA Instruments DIL 801) to obtain the linear shrinkage. This linear shrinkage obtained on individual pellets for different heating rates was then converted to the relative density (ρ_r) using Eq. 2:

$$\rho_r=\frac{1}{\left(1+\frac{\Delta L}{L}\right)^3}\rho_g \qquad (2)$$

where ρ_g is green density and $\Delta L/L$ linear shrinkage.

Relative density as a function of temperature so obtained, was fed to the program developed by Teng *et al*. [16]. The program constructed MSC for $La_2Ti_2O_7$ ceramics upon estimation of the apparent activation energy of sintering. It also provided a combination of time and temperature required during isothermal sintering to obtain various levels of densification. By taking into consideration the time and temperature for isothermal sintering estimated by this program, the validation of MSC was carried out by performing isothermal sintering between 1350–1425 °C for 4 h in a high temperature muffle furnace (Therelek 1700). The microstructure of the ceramics densified for master sintering curve construction was studied using a scanning electron microscope (SEM: Zeiss sigma model). The relative density of ceramics sintered isothermally for MSC validation as well as constant heating rate method for microstructure evolution was determined using the Archimedes' method as per ASTM C 373-88 [17].

III. Results and discussion

X-ray diffraction study was carried out to identify the phase formed due to the solid-state reaction between La_2O_3 and TiO_2 (Fig. 1). The phase identified in this study was monoclinic, as expected. The Rietveld refinement (Fig. 1) carried out with the JCPDS reference file 00-028-0517 confirmed the formation of a single-phase structure [18]. Table 1 shows the lattice parameters obtained after the Rietveld refinement, which are in excellent agreement with the standard lattice parameters. XRD study of the sintered pellets (though out of scope of this paper) revealed that the single-phase monoclinic structure was present similarly to the calcined powder.

Since calcination at 1150 °C resulted in the formation of a single-phase monoclinic $La_2Ti_2O_7$, the next imperative thing to be understood was the densification characteristics of the $La_2Ti_2O_7$ ceramics. These included the determination of the onset temperature of sintering, variation of density during sintering and the activation energy of sintering. These parameters were determined by performing constant heating rate experiments in a dilatometer. The green density of each pellet was maintained at 51 TD% (TD: theoretical density). The heating rates were varied between 5–15 °C/min. To understand the microstructural evolution during sintering of $La_2Ti_2O_7$, the pellets were sintered by a constant-rate heating method in the dilatometer in the temperature range of 1200–1450 °C and their microstructure was studied using scanning electron microscopy.

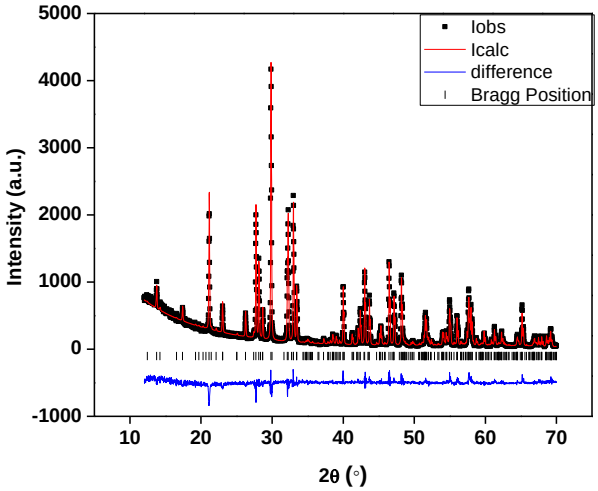

Figure 1. XRD pattern of the calcined $La_2Ti_2O_7$ powder and its Rietveld refinement

Table 1. Comparison of lattice parameters of the calcined $La_2Ti_2O_7$ powder with the standard lattice parameters

Sample	Lattice parameters after Rietveld refinement	Standard lattice parameters	Change [%]
$La_2Ti_2O_7$ powder	a = 7.8168 Å	a = 7.8120 Å	0.06
	b = 5.5498 Å	b = 5.5344 Å	0.27
	c = 13.0224 Å	c = 13.0100 Å	0.10
	$\alpha = \gamma$ = 90°	$\alpha = \gamma$ = 90°	---
	β = 98.68°	β = 98.66°	0.02
	V = 556.07 Å^3	V = 558.43 Å^3	0.42

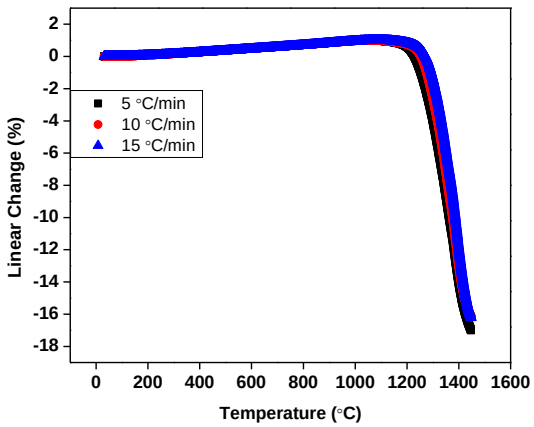

Figure 2. Linear shrinkage of $La_2Ti_2O_7$ pellets during constant rate heating experiment in a dilatometer with heating rates of 5–15 °C/min

Figure 2 shows linear shrinkage of the $La_2Ti_2O_7$ sample as a function of temperature for heating rates of 5–15 °C/min. It can be observed that despite a change in the heating rate, the ceramics followed a similar trajectory during densification and the linear shrinkage of the pellets remained in the range of 16–18%, which is in line with that reported in the literature with other ceramic systems. Moreover, each pellet exhibited an onset sintering temperature of about 1200 °C. The linear shrinkage of the pellets during constant rate heating experiments signifies the densification as a function of temperature. The resultant variation in the density as a function of temperature was determined using the Eq. 2 and shown in Fig. 3. Irrespective of the heating rate, the densification happened similarly, and the final relative density of the pellets was in the range of 90–95 TD% despite varying heating rates from 5 to 15 °C/min.

The green pellets heated with heating rates of 5–15 °C/min indeed followed similar trajectories during

sintering, but they did not overlap. It suggests that heating rates slightly affected the sintering characteristics. Hence, to establish a unified sintering path to determine the relative density as a function of sintering temperature and time, the master sintering curve was constructed. To make MSC, the data for three different rates must be fed into a master sintering curve program. In this study, a Microsoft Excel-based program developed by Teng *et al*. [16] was used. Figure 4 shows the master sintering curve of the $La_2Ti_2O_7$ ceramics, which can be used to estimate the relative density as a function of sintering time and temperature as expressed in terms of θ as per Eq. 1.

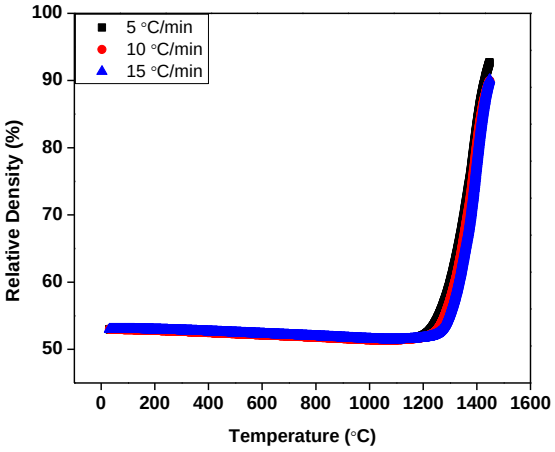

Figure 3. Variation of relative density of pellets as a function of temperature during dilatometric shrinkage study for heating rates of 5–15 °C/min

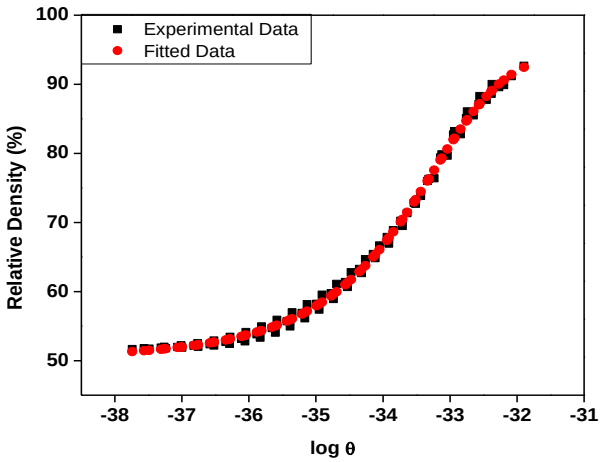

Figure 4. MSC of $La_2Ti_2O_7$ ceramics

Upon estimation of the correct apparent activation energy of sintering, three curves merge into a single curve, a "master sintering curve" that is an excellent tool in estimating the relative density of ceramics as a sintering temperature and time function. The apparent activation energy of sintering determined while constructing the master sintering curve was 1024 kJ/mol. This activation energy corresponds to the least value of the average residual square (Fig. 5).

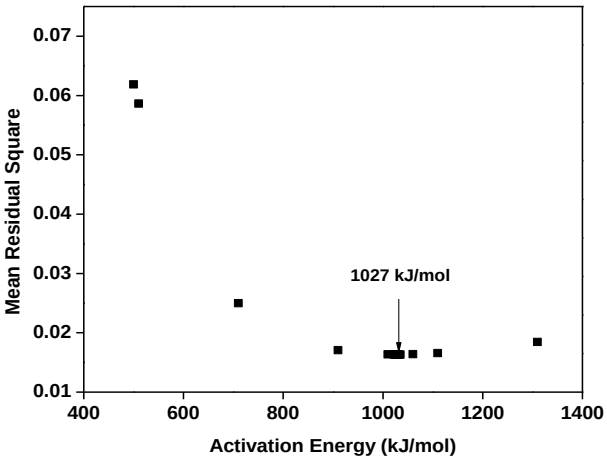

Figure 5. Mean residual square vs. activation energy

Figure 6 shows the microstructure of the pellets sintered by a constant-rate heating method in the dilatometer in the temperature range of 1200–1450 °C. The pellet sintered at 1200 °C shows particles touching each other, whereas the pellet sintered at 1250 °C shows the neck formation between the particles. The microstructural observation with respect to the neck formation is in excellent agreement with the shrinkage experiments wherein the onset of sintering was observed around 1250 °C. With further increase in sintering temperature, the formation of elongated grains has taken place, which is a characteristic feature of $La_2Ti_2O_7$. It can be observed that the increase in sintering temperature caused grain growth in these ceramics, especially for constant rate heating to 1450 °C. Density of the ceramic pellets used for microstructure examination is given in Table 2. It was observed that their density is in line with that determined using dilatometric linear shrinkage data.

The program used to establish the master sintering curve of $La_2Ti_2O_7$ determines the densification achieved for various sintering durations and temperatures, as shown in Table 3. Since the maximum densification achieved in constant rate heating experiments in a dilatometer was 93 TD%, this table provides various combinations of sintering time and temperature for the maximum densification of 93%. Taking the cues from Table 3 and the microstructural evolution, the ceramics were isothermally sintered within a relatively narrow temperature range of 1350–1425 °C for 4 h. The relative density of these pellets as a function of sintering temperature is shown in Fig. 7. The increase in the sintering temperature improved the relative density of ceramics with the maximum relative density reaching almost 99 TD%.

As per the estimations based on the MSC of $La_2Ti_2O_7$, densification above 85 TD% would require

abnormally high isothermal holding time of hundreds or thousands of hours in the temperature range of 1150–1250 °C which can be attributed to the fact that the particles are just touching each other and form necks. This is probably because of surface diffusion effects present in this temperature range which might be hindering diffusion due to its non-densifying nature. However, in the temperature range above 1300 °C, an estimated isothermal holding time of a few hours seems justified. For example, based on Table 3, sintering at 1350 °C for about 7 h would result in the densification of about 93 TD%. The actual isothermal sintering of 1350 °C for 4 h resulted in similar densification. The significant reduction in holding time with respect to that for the temperature range of 1150–1250 °C is an indication that the contribution of densifying mechanisms, such as grain boundary diffusion and lattice diffusion with grain boundary as a source of matter, has increased rather than non-densifying mechanisms, such as surface diffusion [19]. As the estimations shown in Table 3 are restricted to the maximum densification level of 93 TD%, it is not possible to directly compare the densification obtained upon isothermal sintering between 1375–1425 °C. However, based on the trends of estimated densification, some extrapolation is possible. From the Table 3, it can be observed that, for the densification level of 85 TD% and above, the holding time required for the same temperature increases by about 3 times for an incremental density improvement of 3–5%. This phenomenon may be attributed to the grain growth occurring simultaneously along with densification and significant thermal energy being used in grain growth rather than densification alone. This observation can be extrapolated to isothermal sintering at 1400 °C for 4 h which resulted in the densification of about 97 TD% (Fig. 7). According to Table 3, densification at 1400 °C for less than an hour would result in 93% densification. For incremental densification from 93 to 97 TD% at isothermal sintering at 1400 °C, an increase in the holding time to about 4 h is needed.

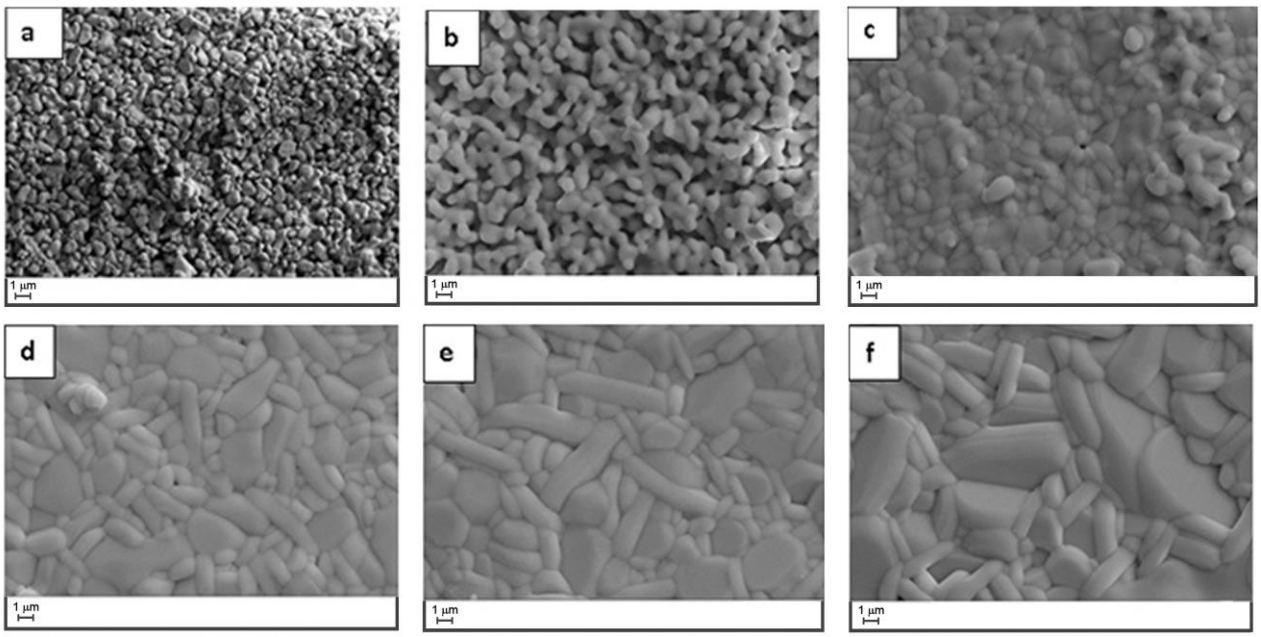

Figure 6. Microstructure of $La_2Ti_2O_7$ ceramics sintered at: a) 1200 °C, b) 1250 °C, c) 1300 °C, d) 1350 °C, e) 1400 °C, f) 1450 °C during dilatometric shrinkage study

Table 2. Density of ceramics sintered by constant rate heating method for microstructure evolution

Temperature [°C]	Relative density [%TD]
1200	52.5
1250	54.3
1300	60.1
1350	71.1
1400	86.2
1450	96.2

It should be noted that while in a maiden attempt to systematically study the densification of $La_2Ti_2O_7$ ceramics, MSC was established, it is restricted to the pressureless sintering of powder obtained by the solid state synthesis route. A change in powder synthesis method from solid state to wet chemical method is likely to lower the onset of sintering temperature and apparent activation energy of sintering due to the smaller particle size and narrow particle size distribution. However, switching to the wet chemical method may have its own set of challenges in terms of raw material prices, storage of raw materials, scalability issues, etc. Similarly, the MSC obtained in this study and associated densification estimations are unlikely to replicate upon changing the sintering

technique to spark plasma sintering, hot pressing, etc. due to different underlying mechanisms.

Table 3. Predicted densification of $La_2Ti_2O_7$ ceramics as a function of temperature and time (in seconds) from master sintering curve

Temperature	Relative density								
[°C]	55 TD%	60 TD%	65 TD%	70 TD%	75 TD%	80 TD%	85 TD%	90 TD%	93 TD%
	Corresponding time in isothermal holding [s]								
1150	1.37×10^5	1.17×10^6	4.07×10^6	1.03×10^7	2.25×10^7	4.74×10^7	1.05×10^8	3.03×10^8	9.44×10^8
1200	7.52×10^3	6.41×10^4	2.23×10^5	5.63×10^5	1.23×10^6	2.60×10^6	5.76×10^6	1.66×10^7	5.17×10^7
1250	499	4.25×10^3	1.48×10^4	3.74×10^4	8.20×10^4	1.72×10^5	3.82×10^5	1.10×10^6	3.43×10^6
1300	39.4	336	1.17×10^3	2.95×10^3	6.47×10^3	1.36×10^4	3.02×10^4	8.70×10^4	2.71×10^5
1350	3.64	31.0	108	273	598	1.26×10^3	2.79×10^3	8.04×10^3	2.50×10^4
1400	0.388	3.31	11.5	29.1	63.8	134	297	857	2.67×10^3
1450	0.0472	0.402	1.40	3.53	7.75	16.3	36.2	104	325

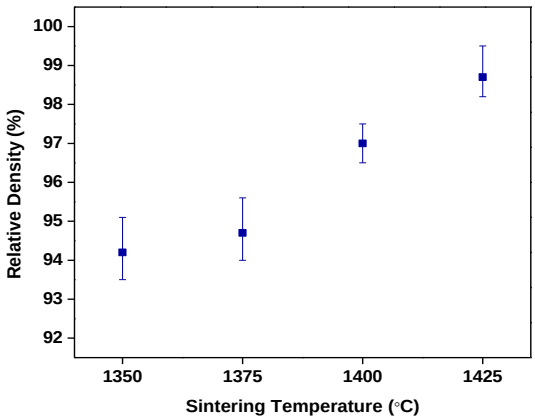

Figure 7. Variation of relative density of $La_2Ti_2O_7$ ceramics as a function of sintering temperature

It is to be noted that the following phenomenological kinetic grain growth equation is not applicable in $La_2Ti_2O_7$:

$$G^n - G_0^{\,n} = K_0 t \exp\left(-\frac{Q}{RT}\right) \quad (3)$$

where, G is the average grain size for a specified sintering time, G_0 is the initial grain size, K_0 is pre-exponential exponent, t is time of sintering, Q is the apparent activation energy, R is universal gas constant, T is absolute temperature and n is grain growth exponent useful in determination of associated diffusion mechanism [20]. The inherent nature of perovskite layer-structured ceramics to exhibit an elongated grain structure poses a challenge in determining associated sintering mechanisms in various temperature regimes [11–13]. As a result, while the apparent activation energy was determined by MSC construction, it is likely that distinct diffusion mechanisms are operative in different temperature regimes with differences in their associated activation energies. Moreover, further research is required regarding activation energies of constituent species during sintering of $La_2Ti_2O_7$ to determine the rate-controlling species.

IV. Conclusions

Single-phase $La_2Ti_2O_7$ powder was synthesized by solid state reaction between La_2O_3 and TiO_2. XRD study confirmed the formation of single-phase monoclinic powders. The master sintering curve (MSC) depicting the pressureless sintering of these ceramics was constructed successfully. The apparent activation energy of sintering determined in the process of construction of MSC was 1027 kJ/mol. The microstructure of the ceramics sintered by the constant rate heating method in a dilatometer were in excellent agreement with the shrinkage data in terms of neck formation, densification and grain growth. Time-temperature estimations based on MSC are useful for designing the pressureless sintering cycles of $La_2Ti_2O_7$ ceramics.

Acknowledgement: Authors, especially KRK, is grateful to Prof. Mao-Hua Teng for providing the computer program for the construction of the master sintering curve.

References

1. H. Su, D.L. Johnson, “Master sintering curve: A practical approach to sintering”, *J. Am. Ceram. Soc.*, **79** (1996) 3211–3217.
2. W.Q. Shao, S.O. Chen, D. Li, Y. Wan, Y.C. Zhang, S.S. Zhang, H.S. Cao, “Analysis of two grain size α-Al_2O_3 sintering at low heating rate based on master sintering curves”, *Mater. Sci. Technol.*, **24** (2008) 734–738.
3. D. Li, S.O. Chen, X.Q. Sun, W.Q. Shao, Y.C. Zhang, S.S. Zhang, “Construction and validation of master sintering curve for TiO_2 for pressureless sintering”, *Adv. Appl. Ceram.*, **107** [1] (2008) 52–56.
4. A. Ray, J. Banerjee, T.R.G. Kutty, A. Kumar, S. Banerjee, “Construction of master sintering curve of ThO_2 pellets using optimization technique”, *Sci. Sinter.*, 44 (2012) 147–160.
5. S. Mitra, A.R. Kulkarni, O. Prakash, “Densification behaviour and two-stage master sintering curve in lithium sodium niobate ceramics”, *Ceram. Int.*, **39** (2013) S65–S68.

6. P.T. Nivala, S.P. James, “Master sintering curves of nickel-titanium and nickel-titanium open-cell foams fabricated by spark plasma sintering”, *J. Mater. Sci.*, **55** (2020) 3668–3683.
7. I.D. Jung, S. Ha, S.J. Park, D.C. Blaine, R. Bollina, R.M. German, “Two-phase master sintering curve for 17-4 PH stainless steel”, *Metall. Mater. Trans. A*, **47** (2016) 5548–5556.
8. T. Frueh, I.O. Ozer, S.F. Poterala, H. Lee, E.R. Kupp, C. Compson, J. Atria, G.L. Messing, “A critique of master sintering curve analysis”, *J. Eur. Ceram. Soc.*, **38** (2018) 1030–1037.
9. S. Nanamatsu, M. Kimura, K. Doi, S. Matsushita, N. Yamada, “A new ferroelectric: $La_2Ti_2O_7$”, *Ferroelectrics*, **8** (1973) 511–513.
10. S. Zhang, F. Yu, “Piezoelectric materials for high-temperature sensors”, *J. Am. Ceram. Soc.*, **94** [10] (2011) 3153–3170.
11. H. Yan, H. Ning, Y. Kan, P. Wang, M.J. Reece, “Piezoelectric ceramics with super-high Curie points”, *J. Am. Ceram. Soc.*, **92** (2009) 2270–2275.
12. Z. Xiong, Z. Gao, S. Li, Q. He, Z. Yang, H. Yan, J. Li, “Pressure-induced structure distortion in ferroelectrics with high Curie point and enhanced piezoelectric properties”, *J. Alloys Compd.*, **818** (2020) 152867.
13. Z. Gao, T.S. Suzuki, S. Grasso, Y. Sakka, M.J. Reece, “Highly anisotropic single crystal-like $La_2Ti_2O_7$ ceramic produced by combined magnetic field alignment and templated grain growth”, *J. Eur. Ceram. Soc.*, **35** (2015) 1771–1776.
14. J.Y. Li, R.C. Rogan, E. Üstündag, K. Bhattacharya, “Domain switching in polycrystalline ferroelectric ceramics”, *Nat. Mater.*, **4** (2005) 776–781.
15. J.L. Jones, B.J. Iverson, K.J. Bowman, “Texture and anisotropy of polycrystalline piezoelectrics”, *J. Am. Ceram. Soc.*, **90** (2007) 2297–2314.
16. M.H. Teng, Y.C. Lai, Y.T. Chen, “A computer program of master sintering curve model to accurately predict sintering results”, *West. Pac. Earth Sci.*, **2** (2002) 171–180.
17. ASTM C-373-88, *Standard Test Method for Water Absorption, Bulk Density, Apparent Porosity, and Apparent Specific Gravity of Fired Whiteware Products*, ASTM International, 2006.
18. National Bureau of Standards (US), *JCPDS Powder Diffraction File-2 00–028–0517*, 2004.
19. M.N. Rahaman, *Ceramic Processing and Sintering*, 2nd ed., Marcel Dekker, New York 2016.
20. M.I. Mendelson, “Average grain size in polycrystalline ceramics”, *J. Am. Ceram. Soc.*, **53** (1969) 443–446.